Article:
Teng, L., Wang, Q., Chen, H. et al. (2021) Atomic norm-based DOA estimation with sum and difference co-arrays in coexistence of circular and non-circular signals. Circuits, Systems, and Signal Processing, 40 (10). pp. 5033-5053. ISSN: 0278-081X

https://doi.org/10.1007/s00034-021-01708-7

Circuits, Systems, and Signal Processing manuscript No.

Atomic Norm Based DOA Estimation with Sum and Difference Co-arrays in Coexistence of Circular and Non-Circular Signals

Liping Teng[1] · Qing Wang [1] · Hua Chen[2*] · Wei Liu [3] · Wei-Ping Zhu[4] · Jingjing Cai[5]

Received: date / Accepted: date

Abstract Sparse arrays can increase the array aperture and degrees of freedom (DOFs) through the construction of either sum or difference co-arrays or both. In order to exploit the advantages of sparse arrays while estimating directions of arrival (DOAs) of a mixture of circular and non-circular signals, in this paper, a gridless DOA estimation method is proposed by employing a recently introduced enhanced nested array, whose virtual arrays have no holes. The virtual signals derived from both sum and difference co-arrays are constructed based on atomic norm minimization. It is shown that the proposed

Liping Teng
tlp512@tju.edu.cn
Qing wang
wangq@tju.edu.cn
Hua Chen (*Corresponding author)
dkchenhua0714@hotmail.com
Wei Liu
w.liu@sheffield.ac.uk
Wei-Ping Zhu
weiping@ece.concordia.ca
Jingjing Cai
jjcai@mail.xidian.edu.cn

1 Schcol of Electrical and Information Engineering, Tianjin University, Tianjin 300072, China.
2* Faculty of Information Science and Engineering, Ningbo University, Ningbo 315211, China.
3 Department of Electronic and Electrical Engineering, The University of Sheffield, Sheffield S1 3JD, UK.
4 Department of Electrical and Computer Engineering, Concordia University, Montreal QC H3G 1M8, Canada.
5 Department of Electronic Engineering, Xidian University, Xian 710071, China.

Part of the work in this paper has been published by 11th IEEE Sensor Array and Multichannel Signal Processing Workshop (SAM 2020) conference [31].

method also works when the circular and non-circular signals come from the same set of directions. Simulation results are provided to demonstrate the performance of the proposed method.

Keywords DOA estimation · Enhanced nested array · Virtual array · Atomic norm · Non-circular signals

1 Introduction

Direction of arrival (DOA) estimation is a key topic in array signal processing, which plays an important role in radar, sonar, navigation, geophysics, acoustic tracking and many other applications [37]. Moreover, considering that both circular and non-circular signals may coexist in real-world applications, the DOA estimation of mixed signals has attracted a lot of research interest recently.

Most of previous methods assume explicitly or implicitly that the source signals are circular. Many approaches have been proposed for DOA estimation of circular or non-circular signals, the subspace-based methods in [6, 24, 25, 27, 28, 33]and the compressive sensing based methods in [11, 17, 18]. Considering that both circular and non-circular signals coexist, in [4, 5], an ESPRIT-like joint diagonalization method was proposed with uniform arrays for a mixture of circular and strictly non-circular sources. In [3], a new data vector was constructed by combining the received uniform array data with its conjugate counterparts. In [10], a DOA estimation method was developed by concatenating the original data and its conjugate; however, this method does not work when the directions of circular and non-circular sources are the same. In [12], a method based on circularity difference was proposed which can realize the estimation of the same DOA for mixed signals and it is suitable for uniform arrays. In [35], polarization channel estimation was achieved for a mixture of circular and non-circular signals based on the unconjugated covariance matrix and covariance matrix differrencing, respectively. In [2], subspace and compressive sensing based methods were proposed to achieve DOA estimation of non-circular signals among mixed sources; however, this method cannot separate circular and non-circular signals.

Sparse arrays can increase the array aperture and degrees of freedom (DOFs) through virtual array generation [26, 43]. Nested array and coprime array are two well-studied sparse array structures, with their number of DOFs given in a closed-form expression. The nested array composed of two ULAs as proposed in [19] can generate a virtual ULA with no holes. Since this specific nested array is susceptible to mutual coupling given its close sensor spacing, a new class of nested arrays was proposed in [13, 14], which can increase DOFs and reduce mutual coupling, but their sum co-arrays have holes. In [32], the coprime array was proposed with reduced mutual coupling; however, its number of DOFs is smaller than nested arrays given the same number of sensors [41]. A generalized coprime array was presented in [22], which can increase DOFs and extend the consecutive part of the virtual array. A thinned coprime array with

reduced mutual coupling was propsed in [23]. In [40], a new method for two-dimensional DOA estimation using two parallel nested arrays was proposed based on augmented covariance matrix with two parallel difference coarrays. Yet it is generally not attractive compared to the nested array and its virtual array also has holes. Since the virtual array derived from sparse arrays usually has holes, for those DOA estimation algorithms designed based on ULAs, only the consecutive part of the virtual co-array can be employed or some interpolation operation has to be performed to fill the holes of the virtual array, which unavoidably leads to different degrees of performance loss. Therefore, it is very important for effective DOA estimation to construct a sparse array whose sum and difference co-arrays have no holes. Recently, a nested array with uniform sum and difference co-arrays was proposed in [9], which provides a basis for further exploring DOA estimation methods using sum and difference co-arrays.

In this paper, we focus on the DOA estimation problem for a mixture of circular and non-circular signals based on sparse arrays and sparse signal representation (SSR). In SSR, the signal parameter space is continuous, and thus the mesh of parameter space will cause the base mismatches [7]. To avoid this problem, some gridless methods have been proposed for DOA estimation. In [15], the Toeplitz matrix was reconstructed based on nuclear norm minimization and interpolation for the difference co-array. In [39], an efficient approach is proposed for estimating the directions-of-arrival (DOAs) of coherent signals using coprime arrays interpolation, in which the Toeplitz matrix is recovered by solving a nuclear norm minimization problem. In [36], a low-rank matrix reconstruction (LRMR) approach was developed with the rank norm replaced by the nuclear norm. For 2-D DOA estimation with an L-shaped sparse array, a gridless method based on a virtual selection matrix and atomic norm was proposed in [38]. A virtual array interpolation-based algorithm for coprime array DOA estimation was proposed in [42], where the atomic norm of the second-order virtual array signals was defined based on the interpolated virtual array. Although gridless DOA estimation methods based on sparse array interpolation are widely used, one prominent issue is that the virtual signals in holes cannot be accurately represented.

In this paper, a DOA estimation method is developed based on atomic norm minimization, which can even work when the circular and non-circular signals come from the same directions. The enhanced nested array proposed in [9] is employed here for DOA estimation as a representative example for the first time in the studied area, given its unique ability of generating no-holes virtual difference and sum co-arrays.

The paper is organized as follows. In Section 2, the model for the coexistence of circular and non-circular signals is introduced and the construction of different sparse arrays is presented including coprime arrays, nested arrays, and enhanced nested arrays. In Section 3, the proposed DOA estimation algorithm is presented. Section 4 analyzes the degree of freedoms and the Cramér–Rao bound. Simulation results are provided in Section 5 and conclusions are drawn in Section 6.

Notations: $\otimes$, $||\cdot||_{\mathcal{A}}$ and $||\cdot||_F$ denote the Kronecker product, atomic norm and frobenius norm, respectively. $(\cdot)^{\mathrm{H}}$, $(\cdot)^{\mathrm{T}}$ and $(\cdot)^*$ respectively stand for conjugate transpose, transpose and complex conjugation. The symbol $\mathrm{E}(\cdot)$ represents the statistical expectation, $diag(\cdot)$ denotes a diagonal matrix generated by the involved elements and $vec(\cdot)$ stands for the vectorization of a martix.

2 Signal Model and Problem Formulation

In this section, we introduce the signal model and the construction methods of different sparse arrays, including coprime array, nested array, and the array used in this paper - enhanced nested array. The virtual arrays generated by different sparse arrays are also compared.

2.1 Signal Model

A complex signal s could be described by its first-order statistics like statistical expectation $\mathrm{E}(s)$, and second-order statistics including autocorrelation covariance $\mathrm{E}(ss^*)$ and elliptic covariance $\mathrm{E}(ss)$. If the non-circularity rate of a complex signal is 0, and its elliptic covariance is also 0, i.e., the square expectation of the magnitude of the in-phase component is the same as that of the orthogonal component, then the signal is a circular signal. If the non-circularity rate is between 0 and 1 and the elliptic covariance is not 0, it is a non-circular signal with non-circularity characteristics [8, 20].

Consider a sparse array $\mathcal{S}$, consisting of N sensors spaced by integer multiples of d, with N being an integer and d being half wavelength, i.e $d = \lambda/2$. Assume there are K_{nc} non-circular and K_c circular narrow-band uncorrelated far field sources from directions $\theta = [\theta_{nc,1}, \theta_{nc,2}, \ldots, \theta_{nc,K_{nc}}, \theta_{c,1}, \theta_{c,2}, \ldots, \theta_{c,K_c}]$. The source signals can be expressed in a vector form as

$$\mathbf{s}(t) = \begin{bmatrix} \mathbf{s}_{nc}(t) \\ \mathbf{s}_c(t) \end{bmatrix}, \tag{1}$$

where

$$\mathbf{s}_{nc}(t) = [s_{nc,1}(t), s_{nc,2}(t), \ldots s_{nc,K_{nc}}(t)]^{\mathrm{T}}, \tag{2}$$

$$\mathbf{s}_c(t) = [s_{c,1}(t), s_{c,2}(t), \ldots s_{c,K_c}(t)]^{\mathrm{T}}. \tag{3}$$

The signals received by the sparse array $\mathcal{S}$ can be expressed as

$$\mathbf{x}(t) = \mathbf{A}\mathbf{s}(t) + \mathbf{n}(t), \tag{4}$$

where, $\mathbf{n}(t)$ is the independent and identically distributed zero-mean additive white Gaussian noise vector, $\mathbf{n}(t) \sim \mathcal{CN}(\mathbf{0}, p_n\mathbf{I})$ with p_n being the noise power

and $\mathbf{I}$ is the identity matrix, and $\mathbf{A}$ represents the array manifold matrix given by

$$\mathbf{A} = [\mathbf{A}_{nc}, \mathbf{A}_c] \in C^{N \times K}, \tag{5}$$

with

$$\mathbf{A}_{nc} = [\mathbf{a}(\theta_{nc,1}), \mathbf{a}(\theta_{nc,2}), \dots \mathbf{a}(\theta_{nc,K})] \in C^{N \times K_{nc}}, \tag{6}$$

$$\mathbf{A}_c = [\mathbf{a}(\theta_{c,1}), \mathbf{a}(\theta_{c,2}), \dots \mathbf{a}(\theta_{c,K})] \in C^{N \times K_c}. \tag{7}$$

where $\mathbf{a}(\theta_k)$ represents the steering vector of the kth source, with $k \in [1, 2, \dots K]$, $K = K_{nc} + K_c$.

The covariance matrix of the received signals is given by

$$\mathbf{R}_{\mathcal{S}} = \mathrm{E}[\mathbf{x}(t)\mathbf{x}^{\mathrm{H}}(t)] = \sum_{k=1}^{K} p_k \mathbf{a}(\theta_k)\mathbf{a}^{\mathrm{H}}(\theta_k) + p_n \mathbf{I}, \tag{8}$$

where p_k is the power of source signals.

The pseudo covariance matrix of the received array signals is given by [2]

$$\mathbf{R}_{\mathcal{S}}^{'} = \mathrm{E}[\mathbf{x}(t)\mathbf{x}^{\mathrm{T}}(t)] = \sum_{k=1}^{K} \rho_k e^{j\varphi_k} p_k \mathbf{a}(\theta_k)\mathbf{a}^{\mathrm{T}}(\theta_k). \tag{9}$$

where φ_k is the non-circularity phase and ρ_k is the non-circularity rate; for non-circular signals, $0 < \rho_k \leq 1$ and for circular signals, $\rho_k = 0$. Therefore, the pseudo covariance matrix contains only the information of non-circular signals, since the corresponding elements are zero for circular signals. For the covariance matrix, both circular and non-circular signals contribute both non-zero components [2].

In practice, the covariance and pseudo covariance matrices are normally replaced by their finite sample approximation as follows

$$\hat{\mathbf{R}}_{\mathcal{S}} = \frac{1}{L} \sum_{t=1}^{L} \mathbf{x}(t)\mathbf{x}^{\mathrm{H}}(t), \tag{10}$$

$$\hat{\mathbf{R}}_{\mathcal{S}}^{'} = \frac{1}{L} \sum_{t=1}^{L} \mathbf{x}(t)\mathbf{x}^{\mathrm{T}}(t). \tag{11}$$

where L is the number of snapshots.

2.2 Sparse Array Construction

The construction methods of the nested array, coprime array and enhanced nested array are introduced below.

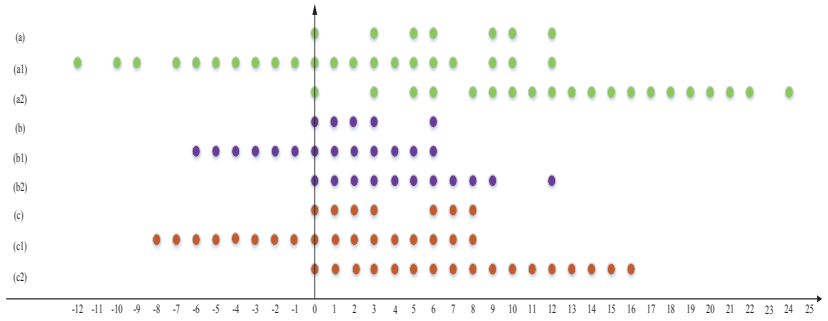

Fig. 1 Sparse array and virtual array construction. (a) Coprime array [42], M=3, N=5. (a1) Difference co-array of the coprime array. (a2) Sum co-array of the coprime array. (b) Nested array [9], N1=3, N2=3. (b1) Difference co-array of the nested array. (b2) Sum co-array of the nested array. (c) ENested array [9], N=9, N1=3, N2=3. (c1) Difference co-array of the ENested array. (c2) Sum co-array of the ENested array.

2.2.1 Coprime array

The coprime array is composed of two ULAs, with M and N sensors, respectively [42]. The position set of the coprime array can be expressed as

$$\begin{aligned} \mathcal{S}_{coprime} = &\{nMd | n = 0, 1, \ldots\ldots N-1\} \\ &\cup \{nNd | n = 0, 1, \ldots\ldots M-1\}, \end{aligned} \tag{12}$$

where M and N are coprime integers and the total number of sensors is $M + N - 1$. Fig. 1(a) shows the coprime array with $M = 3$ and $N = 5$ as an example.

2.2.2 Nested array

The two-level nested array is composed of two linear arrays, with N_1 and N_2 sensors, respectively [9]. The the position set can be expressed as

$$\begin{aligned} \mathcal{S}_{nested} = &\{nd | n = 0, 1, \ldots\ldots N_1 - 1\} \\ &\cup \{nN_1 d | n = 0, 1, \ldots\ldots N_2 - 1\}, \end{aligned} \tag{13}$$

where N_1 and N_2 are integers and the total number of sensors is $N_1 + N_2 - 1$, Fig. 1(b) shows the nested array with $N_1 = 3$ and $N_2 = 3$ as an example.

2.2.3 Enhanced nested array (ENested array)

The ENested array composed of the nested array and an additional array [9] has the following position set

$$\begin{aligned} \mathcal{S}_{ENested} = &\{n | n = 0, 1, \ldots\ldots N_1 - 1\} \\ &\cup \{nN_1 | n = 0, 1, \ldots\ldots N_2 - 1\} \\ &\cup \{n | n = N - N_1, \ldots\ldots N - 1\} \end{aligned}. \tag{14}$$

Fig. 1(c) shows the ENested array with $N_1 = 3$, $N_2 = 3$ and $N = 9$ as an example.

2.3 Virtual Array Construction

Sparse array increases the degrees of freedom through the generation of difference co-array and/or sum co-array, which are defined as follows.

Definition 1 (*Difference co-array*) For sparse array $\mathcal{S}$, the difference co-array is defined as $\tilde{\mathcal{U}}_{diff} = \{n - m | n, m \in \mathcal{S}\}$, and then $\mathcal{U}_{diff}$ is defined as the distinct elements in the position set $\tilde{\mathcal{U}}_{diff}$.

Definition 2 (*Sum co-array*) For sparse array $\mathcal{S}$, the sum co-array is defined as $\tilde{\mathcal{U}}_{sum} = \{n + m | n, m \in \mathcal{S}\}$, and then $\mathcal{U}_{sum}$ is defined as the distinct elements in the position set $\tilde{\mathcal{U}}_{sum}$.

The difference and sum co-arrays of coprime array, nested array and ENested array are shown in Fig. 1. For the coprime array, the difference and sum co-arrays are both non-uniform arrays as shown in Fig. 1(a1) and Fig. 1(a2). For a non-uniform virtual array, the schemes of extracting central continuous uniform array and virtual array interpolation are adopted for DOA estimation. However, the method of extracting the central continuous uniform array leads to loss of information, while virtual array interpolation cannot accurately represent the signal at the hole positions. As shown in Fig. 1(b1), the differences co-array of the nested array has no holes, while the sum and difference co-arrays of the ENnested array have no holes as shown in Fig. 1(c1) and Fig. 1(c2).

In this paper, we propose a DOA estimation method based on the ENested array in the coexistence of circular and non-circular signals, and show through computer simulation that the proposed method can be applied to any sparse arrays, such as coprime arrays and nested arrays.

3 The Proposed DOA Estimation Method

In this section, we propose an atomic norm minimization based DOA estimation method by employing the ENested array as an example. Firstly, the covariance matrix of the sum co-array signals are reconstructed by minimizing the atomic norm, based on which the DOA of non-circular signals is estimated. Then, the covariance matrix of the circular signals is obtained using the estimated DOA of the non-circular signals, and the difference co-array signals corresponding to the circular signals are derived. Finally, the covariance matrix of the difference co-array signals is obtained using the minimized atomic norm, which is further employed to estimate the DOA of the circular signals.

3.1 DOA Estimation of Non-circular Signals

Considering the coexistence of circular and non-circular signals, we can rewrite the pseudo covariance matrix in Eq. (9) as

$$\mathbf{R}_{\mathcal{S}}^{'} = \mathbf{A}_{nc}\mathbf{R}_{nc}^{'}\mathbf{A}_{nc}^{\mathrm{T}} + \mathbf{A}_{c}\mathbf{R}_{c}^{'}\mathbf{A}_{c}^{\mathrm{T}}, \tag{15}$$

where $\mathbf{R}_{nc}^{'} = \mathrm{E}[\mathbf{s}_{nc}\mathbf{s}_{nc}^{\mathrm{T}}]$ and $\mathbf{R}_{c}^{'} = \mathrm{E}[\mathbf{s}_{c}\mathbf{s}_{c}^{\mathrm{T}}]$. Since the non-circular ratio of the circular signal $\rho_k = 0$, we have $\mathbf{R}_{c}^{'} = 0$. Accordingly, the pseudo-covariance only contains non-circular information. When the directions of circular signals and non-circular signals are the same, the pseudo-covariance can be used to estimate the non-circular signal DOA first, and then the circular signal DOA can be estimated by using the covariance. Thus, Eq. (15) is simplified as

$$\mathbf{R}_{\mathcal{S}}^{'} = \mathbf{A}_{nc}\mathbf{R}_{nc}^{'}\mathbf{A}_{nc}^{\mathrm{T}}. \tag{16}$$

By vectorizing $\mathbf{R}_{\mathcal{S}}^{'}$, we have

$$\mathbf{y}_{\tilde{\mathcal{U}}_{sum}} = vec(\mathbf{R}_{\mathcal{S}}^{'}) = \sum_{k=1}^{K_{nc}} \rho_k e^{j\varphi_k} p_k \mathbf{a}_{nc}^{'}(\theta_k), \tag{17}$$

where

$$\mathbf{a}'_{nc}(\theta_k) = \mathbf{a}_{nc}(\theta_k) \otimes \mathbf{a}_{nc}(\theta_k). \tag{18}$$

The virtual array signals of sum co-array can be selected from vector $\mathbf{y}_{\tilde{\mathcal{U}}_{sum}}$

$$\mathbf{y}_{\mathcal{U}_{sum}} = \sum_{k=1}^{K_{nc}} \rho_k p_k e^{j\varphi_k} \mathbf{v}_{nc}(\theta_k), \tag{19}$$

where $\mathbf{v}_{nc}(\theta_k)$ is the equivalent steering vector chosen from $\mathbf{a}'_{nc}(\theta_k)$, as $\mathcal{U}_{sum}$ is defined as the distinct elements in the position set $\tilde{\mathcal{U}}_{sum}$.

Inspired by the atomic norm theory [1, 30], we absorb the non-circular phase φ_k and $e^{j\varphi_k}$ into the following atomic set

$$\mathcal{A} = \{\mathbf{v}(\theta_k, \varphi_k)\,|\theta_k \in [-90^\circ, 90^\circ], \varphi_k \in [0^\circ, 180^\circ]\,\}. \tag{20}$$

where $\mathbf{v}(\theta_k, \varphi_k) = e^{j\varphi_k}\mathbf{v}_{nc}(\theta_k)$.

The virtual measurements can be expressed in the form of atomic norm minimization as follows

$$\|\mathbf{y}_{\mathcal{U}_{sum}}\|_{\mathcal{A}} = \inf_{\rho_k, p_k} \left\{ \begin{array}{l} \sum\limits_{k=1}^{K_{nc}} \rho_k p_k : \\ \mathbf{y}_{\mathcal{U}_{sum}} = \sum\limits_{k=1}^{K_{nc}} \mathbf{v}(\theta_k, \varphi_k)\rho_k p_k, \\ p_k \geq 0, 0 < \rho_k \leq 1. \end{array} \right\}. \tag{21}$$

Eq. (21) can be expressed as an equivalent optimal solution to the following semi-definite programming (SDP) problem [1]

$$\begin{aligned} \min_{\mathcal{T},u} \frac{1}{2}u + \frac{1}{2N_{\mathcal{U}_{sum}}} Tr\left[\mathcal{T}'\right], \\ s.t. \begin{bmatrix} u & \mathbf{y}_{\mathcal{U}_{sum}}^{\mathrm{H}} \\ \mathbf{y}_{\mathcal{U}_{sum}} & \mathcal{T}' \end{bmatrix} \geq 0, \end{aligned} \tag{22}$$

where $\mathcal{T}'$ is a Hermitian Toeplitz matrix,

$$\mathcal{T}' = \sum_{k=1}^{K_{nc}} \rho_k p_k \mathbf{v}(\theta_k, \varphi_k)\mathbf{v}^{\mathrm{H}}(\theta_k, \varphi_k), \tag{23}$$

and $N_{\mathcal{U}_{sum}}$ denotes the number of sensors in the sum co-array.

We plug $\mathbf{v}(\theta_k, \varphi_k) = e^{j\varphi_k}\mathbf{v}_{nc}(\theta_k)$ into Eq. (23) to obtain

$$\begin{aligned} \mathcal{T}' &= \sum_{k=1}^{K_{m,}} \rho_k p_k \left(\mathbf{v}\left(\theta_k\right) e^{j\varphi_k}\right)\left(\mathbf{v}\left(\theta_k\right) e^{j\varphi_k}\right)^{\mathbf{H}} \\ &= \sum_{k=1}^{K_{u_k}} \rho_k p_k \mathbf{v}\left(\theta_k\right)\left(\mathbf{v}\left(\theta_k\right)\right)^{\mathbf{H}} \end{aligned} \tag{24}$$

According to Eq. (24), the matrix $\mathcal{T}'$ corresponding to the atomic set containing θ_k and φ_k is the same as the matrix $\mathcal{T}'$ corresponding to the atomic set only containing θ_k, that is, $\mathcal{T}'$ solved after SVD will not have the effect of non-circular phase φ_k.

Taking the error into account in the SDP constraints, the optimization problem in Eq. (22) can be expressed as

$$\begin{aligned} \min_{\mathcal{T},u} \frac{1}{2}u + \frac{1}{2N_{\mathcal{U}_{sum}}} Tr\left[\mathcal{T}'\right], \\ s.t. \begin{bmatrix} u & \mathbf{y}_{\mathcal{U}_{sum}}^{\mathrm{H}} \\ \mathbf{y}_{\mathcal{U}_{sum}} & \mathcal{T}' \end{bmatrix} \geq 0, \\ \left\|\hat{\mathbf{y}}_{\mathcal{U}_{sum}} - \mathbf{y}_{\mathcal{U}_{sum}}\right\|_2^2 \leq \varepsilon \end{aligned} \tag{25}$$

where ε upper-bounds the fitting error, and $\hat{\mathbf{y}}_{\mathcal{U}_{sum}}$ is obtained by vectorizing the approximate pseudo covariance $\hat{\mathbf{R}}_{\mathcal{S}}^{'}$ and selecting the equivalent value.

The optimization problem Eq. (25) can be further expressed as

$$\begin{aligned} \min_{\mathcal{T},u} \frac{1}{2}u + \frac{1}{2N_{\mathcal{U}_{sum}}} Tr\left[\mathcal{T}'\right] + \frac{1}{2}\left\|\hat{\mathbf{y}}_{\mathcal{U}_{sum}} - \mathbf{y}_{\mathcal{U}_{sum}}\right\|_2^2, \\ s.t. \begin{bmatrix} u & \mathbf{y}_{\mathcal{U}_{sum}}^{\mathrm{H}} \cdot \\ \mathbf{y}_{\mathcal{U}_{sum}} & \mathcal{T}' \end{bmatrix} \geq 0. \end{aligned} \tag{26}$$

Eq. (26) is now convex, and can be solved by the CVX toolbox in MATLAB, and the covariance matrix $\mathcal{T}'$ of the sum co-array is then obtained, which can be used by a MUSIC-type method to estimate DOA $\theta_{nc,k}$ of non-circular signals.

3.2 DOA Estimation of Circular Signals

For estimating the DOA of circular sources, we need to analyse the covariance matrix in Eq. (8), which can be expressed as

$$\mathbf{R}_{\mathcal{S}} = \mathbf{A}_{nc}\mathbf{R}_{nc}\mathbf{A}_{nc}^{\mathrm{H}} + \mathbf{A}_{c}\mathbf{R}_{c}\mathbf{A}_{c}^{\mathrm{H}}, \tag{27}$$

where $\mathbf{R}_{nc} = E[\mathbf{s}_{nc}\mathbf{s}_{nc}^{\mathrm{H}}]$ and $\mathbf{R}_{c} = E[\mathbf{s}_{c}\mathbf{s}_{c}^{\mathrm{H}}]$.

From the DOAs of non-circular signals and Eq. (16), we can obtain $\mathbf{R}_{nc}^{'}$, thereby leading $\mathbf{R}_{nc}$ to [12]

$$\mathbf{R}_{nc} = diag\{\left|R_{nc}^{'}(1,1)\right|, \ldots \left|R_{nc}^{'}(K_{nc},K_{nc})\right|\}, \tag{28}$$

Using $\mathbf{R}_{nc}$, we can estimate the covariance matrix of non-circular signals. The covariance matrix of circular signals can then be obtained by subtracting the non-circular part from Eq. (27) [12], giving

$$\mathbf{R} = \mathbf{R}_{\mathcal{S}} - \mathbf{A}_{nc}\mathbf{R}_{nc}\mathbf{A}_{nc}^{\mathrm{H}}. \tag{29}$$

The difference virtual vector can be obtained by vectorizing $\mathbf{R}$ as

$$\mathbf{y}_{\tilde{\mathcal{U}}_{diff}} = vec(\mathbf{R}) = \sum_{k=1}^{K_c} p_k \mathbf{a}_{c}^{'}(\theta_k) + p_n\mathbf{i}, \tag{30}$$

where

$$\mathbf{a}'_{c}(\theta_k) = \mathbf{a}_{c}^{*}(\theta_k) \otimes \mathbf{a}_{c}(\theta_k). \tag{31}$$

The virtual signals of the difference co-array are obtained from vector $\mathbf{y}_{\tilde{\mathcal{U}}_{diff}}$ as

$$\mathbf{y}_{\mathcal{U}_{diff}} = \sum_{k=1}^{K_c} p_k \mathbf{z}(\theta_k) + p_n\bar{\mathbf{i}}. \tag{32}$$

where $\mathbf{z}(\theta_k)$ is the obtained equivalent steering vector from $\mathbf{a}'_{c}(\theta_k)$.

Based on the atomic norm theory, we have the the atomic set of difference co-array and virtual measurements as follows

$$\mathcal{A} = \{\mathbf{z}(\theta_k)\,|\theta_k \in [-90^{\circ}, 90^{\circ}]\,\}, \tag{33}$$

$$\left\|\mathbf{y}_{\mathcal{U}_{diff}}\right\|_{\mathcal{A}} = \inf_{p_k}\left\{\sum_{k=1}^{K_c} p_k : \mathbf{y}_{\mathcal{U}_{diff}} = \sum_{k=1}^{K_c} p_k\mathbf{z}(\theta_k), p_k \geq 0\right\}. \tag{34}$$

The equivalent SDP form of Eq. (34) is given by

$$\begin{aligned} &\min_{\mathcal{T},t} \frac{1}{2}t + \frac{1}{2N_{\mathcal{U}_{diff}}} Tr\left[\mathcal{T}\right], \\ &s.t. \begin{bmatrix} t & \mathbf{y}_{\mathcal{U}_{diff}}^{\mathrm{H}} \\ \mathbf{y}_{\mathcal{U}_{diff}} & \mathcal{T} \end{bmatrix} \geq 0, \end{aligned} \tag{35}$$

where $\mathcal{T}$ is expressed as

$$\mathcal{T} = \sum_{k=1}^{K_c} p_k \mathbf{z}(\theta_k)\mathbf{z}^{\mathrm{H}}(\theta_k), \tag{36}$$

In Eq. (35), $t = \sum_{k=1}^{K_c} p_k$, and $N_{\mathcal{U}_{diff}}$ denotes the number of sensors of the difference co-array or that of difference co-array with holes.

Considering the error of virtual signals in the SDP constraints, the optimization problem can be finally formulated as

$$\begin{aligned} &\min_{\mathcal{T},t} \frac{1}{2}t + \frac{1}{2N_{\mathcal{U}_{diff}}} Tr\left[\mathcal{T}\right], \\ &s.t. \begin{bmatrix} t & \mathbf{y}_{\mathcal{U}_{diff}}^{\mathrm{H}} \\ \mathbf{y}_{\mathcal{U}_{diff}} & \mathcal{T} \end{bmatrix} \geq 0, \\ &\left\| \hat{\mathbf{y}}_{\mathcal{U}_{diff}} - \mathbf{y}_{\mathcal{U}_{diff}} \right\|_2^2 \leq \varepsilon \end{aligned} \tag{37}$$

where ε provides the upper bound for the fitting error, and $\hat{\mathbf{y}}_{\mathcal{U}_{diff}}$ is obtained by vectoring the approximate covariance matrix $\hat{\mathbf{R}}$ and selecting the equivalent values, and $\hat{\mathbf{R}} = \hat{\mathbf{R}}_{\mathcal{S}} - \mathbf{A}_{nc}\mathbf{R}_{nc}\mathbf{A}_{nc}^{\mathrm{H}}$

The optimization problem in Eq.(37) can be expressed as

$$\begin{aligned} \min_{\mathcal{T},t} \frac{1}{2}t + \frac{1}{2N_{\mathcal{U}_{diff}}} Tr\left[\mathcal{T}\right] + \frac{1}{2}\left\| \hat{\mathbf{y}}_{\mathcal{U}_{diff}} - \mathbf{y}_{\mathcal{U}_{diff}} \right\|_2^2, \\ s.t. \begin{bmatrix} t & \mathbf{y}_{\mathcal{U}_{diff}}^{\mathrm{H}} \\ \mathbf{y}_{\mathcal{U}_{diff}} & \mathcal{T} \end{bmatrix} \geq 0. \end{aligned} \tag{38}$$

Using the CVX toolbox to solve the problem, we can obtain $\mathcal{T}$ and the covariance matrix of the difference co-array signals. Then, MUSIC-type algorithm can then be used to estimate DOAs of circular signals.

4 Performance Analysis

4.1 DOFs

For sparse arrays, we express the DOFs in terms of the number of the maximum consecutive virtual arrays. Since the proposed algorithm makes use of both sum co-array and difference co-array, the DOFs of sum and difference virtual arrays are represented separately. We compare the DOFs of different sparse arrays as follows.

With the position set of coprime array shown in Eq. (12), the total number of sensors is $M + N - 1$. For difference co-array, the maximum position of the positive axis is $MN - M$, while the minimum position of the negative axis is $-(MN - M)$. The maximum consecutive part is thus from $-(M + N - 1)$ to $M+N-1$ and the DOFs are $2(M+N)-1$ [21]. For sum co-array, the maximum

Table 1 DOFs Comparison of Different Arrays.

Type	N_1, N_2	PSN	$(mi, ma)_{diff}$	(MC)D_{diff}	$(mi.ma)_{sum}$	(MC)D_{sum}
Coprime	3,5	7	(-12,12)	(-7,7)15	(0,24)	(8,22)15
Nested	3,3	5	(-6,6)	(-6,6)13	(0,12)	(0,9)10
ENested	3,3	7	(-8,8)	(-8,8)17	(0,16)	(0,16)17
ULA7	/	7	(-6,6)	(-6,6)13	(0,12)	(0,12)13
ULA9	/	9	(-8.8)	(-8,8)17	(0,16)	(0,16)17

position of the positive axis is $2MN - 2M$. The maximum consecutive part is from $(M-1)(N-1)$ to $MN + N - 1$ when $M = 2$ and from $(M-1)(N-1)$ to $MN + +M + N - 1$ when $M > 2$. The DOFs are thus $M + 2N - 1$ when $M = 2$, $2(M + N) - 1$ when $M > 2$ [34].

From the position set of nested array shown in Eq. (13), the total number of sensors is $N_1 + N_2 - 1$. For difference co-array, the maximum position of the positive axis is $N_1N_2 - N_1$, while the minimum position of the negative axis is $-(N_1N_2 - N_1)$. Thus the maximum consecutive part is from $-(N_1N_2 - N_1)$ to $N_1N_2 - N_1$ and the DOFs are $2N_1N_2 - 2N_1 + 1$. For sum co-array, the maximum position of the positive axis is $2N_1N_2 - 2N_1$. The maximum consecutive part is then from 0 to N_1N_2 and the DOFs are $N_1N_2 + 1$.

Considering the position set of Enested array shown in Eq. (14), the total number of sensors is $2N_1 + N_2 - 2$. For difference co-array, the maximum position of the positive axis is $N_1N_2 - 1$, and the minimum position of the negative axis is $-(N_1N_2 - 1)$. The maximum consecutive part is thus from $-(N_1N_2 - 1)$ to $N_1N_2 - 1$ and the DOFs are $2N_1N_2 - 1$. For sum co-array, the maximum position of the positive axis is $2N_1N_2 - 2$. The maximum consecutive part is from 0 to N_1N_2 and the DOFs are $2N_1N_2 - 1$.

By referring to the virtual co-arrays of different sparse arrays shown in Fig. 1, the comparison of sum DOFs and dirrerence DOFs with coprime array, nested array, Enested array, ULAs with 7 sensors and 9 sensors is shown in Table 1. PSN expresses the total number of phsicaly sensors, $(mi, ma)_{diff}$ and $(mi.ma)_{sum}$ are the minimum position of the negative axis and the maximum position of the positive axis for difference and sum co-array, respectively. MC expresses the range of maximum consecutive ULA. And D_{diff} and D_{sum} express the DOFs for difference and sum co-array with different array construction, respectively. Obviously, the Enest array achieves the same DOF as the ULA9 in both sum and difference co-arrays, while the virtual arrays have no holes.

4.2 Cramér–Rao Bound

The Cramér–Rao Bound (CRB) offers a lower bound for unbiased estimates of parameters. For real-valued parameter vector $\alpha = [\bar{\theta}, \mathbf{p}, p_n]^{\mathrm{T}}$, the (i,j)th entry of the Fisher Information Matrix (FIM) is given by [42]

$$[FIM]_{i,j} = Ltr(\mathbf{R}_{\mathcal{S}}^{-1}\frac{\partial \mathbf{R}_{\mathcal{S}}}{\partial [\alpha]_i}\mathbf{R}_{\mathcal{S}}^{-1}\frac{\partial \mathbf{R}_{\mathcal{S}}}{\partial [\alpha]_j}), \tag{39}$$

which is further expressed as

$$[FIM]_{i,j} = L[vec(\frac{\partial \mathbf{R}_{\mathcal{S}}}{\partial [\alpha]_i})^{\mathrm{H}}](\mathbf{R}_S^{-\mathrm{T}} \otimes \mathbf{R}_S^{-1})vec(\frac{\partial \mathbf{R}_{\mathcal{S}}}{\partial [\alpha]_j}), \tag{40}$$

The FIM matrix can be decomposed into [29]

$$FIM = L\begin{bmatrix}\mathbf{G}^H \\ \Delta^H\end{bmatrix}\begin{bmatrix}\mathbf{G} & \Delta\end{bmatrix}. \tag{41}$$

where $\mathbf{G}$ is given by

$$\mathbf{G} = (\mathbf{R}_S^{\mathrm{T}} \otimes \mathbf{R}_{\mathcal{S}})^{-1/2}\begin{bmatrix}\frac{\partial \mathbf{y}}{\partial p_1} & \cdots & \frac{\partial \mathbf{y}}{\partial p_K} & \frac{\partial \mathbf{y}}{\partial p_n}\end{bmatrix}, \tag{42}$$

$$\mathbf{y} = \mathrm{vec}(\mathbf{R}_S), \tag{43}$$

and Δ is given by

$$\Delta = (\mathbf{R}_S^{\mathrm{T}} \otimes \mathbf{R}_S)^{-1/2}[\frac{\partial \mathbf{y}}{\partial \bar{\theta}_1} \cdots \frac{\partial \mathbf{y}}{\partial \bar{\theta}_K}]. \tag{44}$$

According to the derivation of CRB in [16], $\mathbf{G}$ and Δ can be simplified as

$$\mathbf{G} = -j2\pi(\mathbf{R}_{\mathcal{S}}^{\mathrm{T}} \otimes \mathbf{R}_{\mathcal{S}}^{\mathrm{T}})^{-1/2}\mathbf{J}(diag(\mathcal{U}_{diff}))\mathbf{V}_{\mathcal{U}_{diff}}\mathbf{P}, \tag{45}$$

$$\Delta = (\mathbf{R}_{\mathcal{S}}^{\mathrm{T}} \otimes \mathbf{R}_{\mathcal{S}}^{\mathrm{T}})^{-1/2}\mathbf{J}\mathbf{W}, \tag{46}$$

where $\mathbf{V}_{\mathcal{U}_{diff}}$ is array manifold of the difference co-array, $\mathbf{P}$ is the diagonal matrix with signal power and $\mathbf{J}$ is a binary matrix, representing the correspondence between $\tilde{\mathcal{U}}_{diff}$ and $\mathcal{U}_{diff}$

$$\mathbf{V}_{\mathcal{U}_{diff}} = [\mathbf{v}_{\mathcal{U}_{diff}}(\bar{\theta}_1) \cdots \mathbf{v}_{\mathcal{U}_{diff}}(\bar{\theta}_K)], \tag{47}$$

$$\mathbf{P} = diag(p_1, p_2, \cdots p_K), \tag{48}$$

$$\mathbf{W} = \begin{bmatrix}\mathbf{v}_{\mathcal{U}_{diff}}(\bar{\theta}_1) \cdots \mathbf{v}_{\mathcal{U}_{diff}}(\bar{\theta}_K) & \mathbf{i}\end{bmatrix}. \tag{49}$$

Therefore, the CRB can be obtained as [16]

$$CRB(\bar{\theta}) = \frac{1}{4\pi^2 L}(\mathbf{G}_0^{\mathrm{H}}\Pi_{\mathbf{MW}}^{\perp}\mathbf{G}_0^{\mathrm{H}})^{-1}, \tag{50}$$

where

$$\Pi_{\mathbf{MW}}^{\perp} = \mathbf{I} - \mathbf{MW}((\mathbf{MW})^{\mathrm{H}}\mathbf{MW})^{-1}(\mathbf{MW})^{\mathrm{H}}, \tag{51}$$

$$\mathbf{M} = (\mathbf{J}^{\mathrm{H}}(\mathbf{R}_S^{\mathrm{T}} \otimes \mathbf{R}_S^{\mathrm{T}})^{-1}\mathbf{J})^{1/2}, \tag{52}$$

$$\mathbf{G}_0 = \mathbf{M}(diag(\mathcal{U}_{diff}))\mathbf{V}_{\mathcal{U}_{diff}}\mathbf{P}. \tag{53}$$

5 Simulation Results

In our simulation, an Enested array with $N_1 = 3$ and $N_2 = 3$ is used, which has 7 physical sensors with their locations shown in Fig. 1(c). Further the virtual arrays are shown as Fig. 1(c1) and Fig. 1(c2). As a comparison, the coprime array of $M = 3$ and $N = 5$, with 7 physical sensors, and the equivalent signals of sum and difference virtual arrays are obtained via interpolation [42]. Besides, two ULAs with 7 and 9 physical sensors are also considered for comparison.The root mean square errors (RMSEs) with respect to signal-to-noise ratio (SNR) and snapshot number of different sparse arrays are compared based on the proposed method. The RMSE is defined as

$$RMSE = \sqrt{\frac{1}{KM}\sum_{m=1}^{M}\sum_{k=1}^{K}(\hat{\bar{\theta}}_{k,m} - \bar{\theta}_k)^2}, \tag{54}$$

where M stands for the number of Monte Carlo trials, $\hat{\bar{\theta}}_{k,m}$ denotes the normalized DOA estimation result of the kth source at the mth Monte Carlo trial and $\bar{\theta}_k = (d/\lambda)\sin(\theta_k)$.

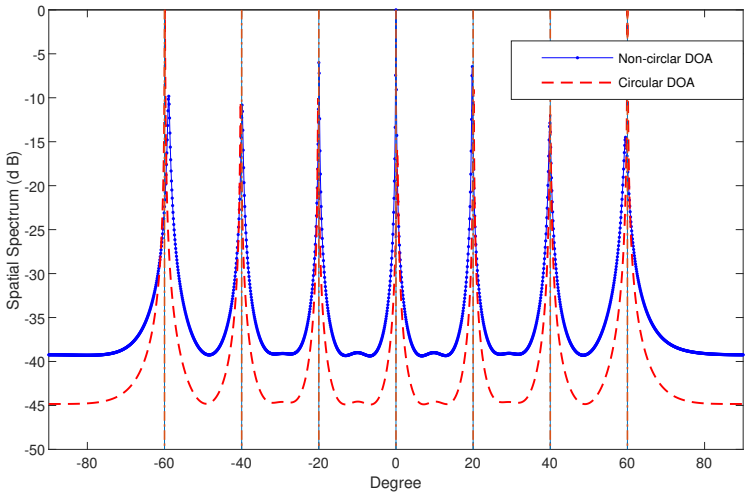

Fig. 2 The spatial spectrum results with same directions.

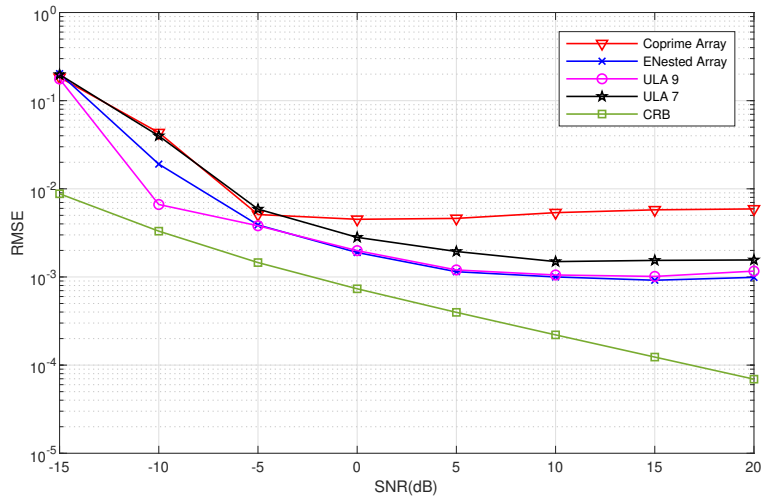

(a)

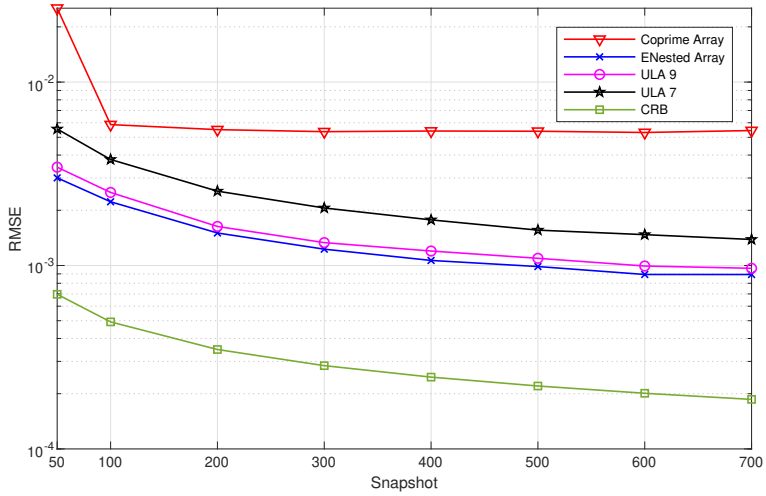

(b)

Fig. 3 RMSE comparison with a different set of directions: 2 circular and 2 non-circular sources. (a) RMSE versus SNR, (b) RMSE versus snapshot number.

In the first example, we consider seven uncorrelated circular sources uniformly distributed in $[-60°, 60°]$, which coincide with seven uncorrelated non-circular sources uniformly distributed in the same range. The spatial spectrum obtained with the seven-sensor ENested array is shown in Fig. 2, with snapshot number $L = 500$ and SNR $= 30dB$. It is observed that proposed algorithm can distinguish the DOAs of circular and non-circular signals from the same directions. This is because the proposed algorithm estimates the non-circular

signals using the sum virtual array firstly, while the difference virtual array is used to estimate the circular signals. The process of estimating the DOAs of circular and non-circular signals is separated. In addition, since both the sum and difference co-arrays are used in the proposed algorithm, the number of distinguishable mixed signals exceeds the number of physical elements.

In the second example, the circular and non-circular signals come from different directions. There are two non-circular sources uniformly distributed in $[-30°, 10°]$, and two circular sources uniformly distributed in $[20°, 70°]$. The RMSE result obtained by 200 Monte Carlo trials with snapshot number $L = 500$ from the ENested array, coprime array, 7-sensor ULA and 9-sensor ULA are shown in Fig. 3(a). Fig. 3(b) shows the RMSE result with respect to the same snapshot number at an SNR of $10dB$. It is observed that the RMSE of the ENested array is close to the 9-sensor ULA which is better than the 7-sensor ULA. This is because the sum and difference co-arrays of the ENested array are the same as the 9-sensor ULA, and achieves a better result at a lower SNR and becomes stable with the increase of SNR. Besides, the DOA estimation result of the coprime array is worse than other arrays due to the holes of its virtual array.

In the third example, we compare the proposed method with the sparse array DOA estimation method proposed in [2]. Since the method in [2] cannot work when the circular and non-circular signals come from the same direction, we consider the case with different directions and give the RMSE of mixture signals. When there are one non-circular source from $10°$ and one circular source from $30°$, the resulting RMSE at SNR $= 10dB$ and 200 Monte Carlo trials is shown in the Fig. 4. By comparing the RMSE of the two methods for both circular and non-circular sources, we can see that overall our proposed method has achieved a better performance than Cai's method in [2]. The reference algorithm estimates directions using a compressed sensing method which based on the meshed parameter space. But since the signal parameter space is continuous, the mesh of parameter space causes base mismatches. In contrast, the proposed method uses on the gridless atomic norm to reconstruct the toeplitz matrix, which can further improve the estimation accuracy.

In the fourth example, we explore the effect of DOA separation. Assume two signals, one circular and one non-circular. The direction of the non-circular signal is $45°$, while the direction of the circular signal varies from $45°$ to $55°$. The RMSE result obtained from $SNR = 10dB$, $L = 500$ and 500 Monte Carlo trials is shown in Fig. 5. Surprisingly, the performance is better when the DOA separation of circular and non-circular signals is smaller. This could be explained as follows. In theory, there is no circular signal information in the pseudo covariance matrix, but in practice, circular signal information could affect the pseudo covariance matrix, and when DOA separation is small, the direction of circular signals is very close to the direction of non-circular signals, so that the additional influence of circular signals on the pseudo covariance matrix is smaller. This could also explain why the estimation performance for the same-DOA is better than the case with different DOAs.

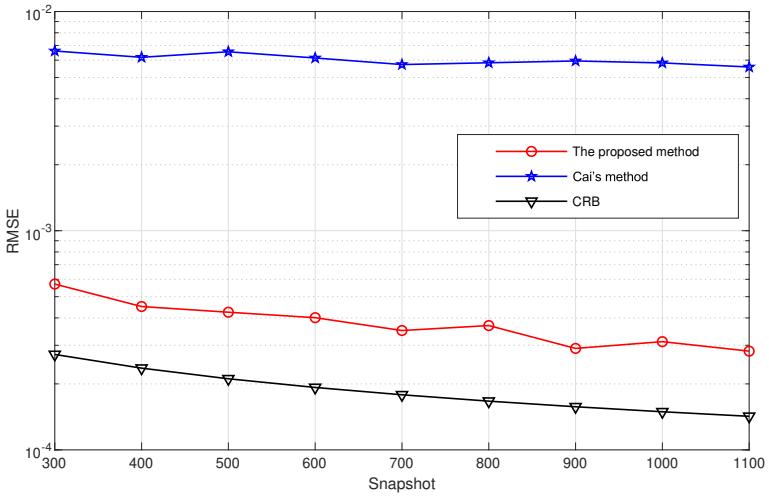

Fig. 4 Comparison of two different methods.

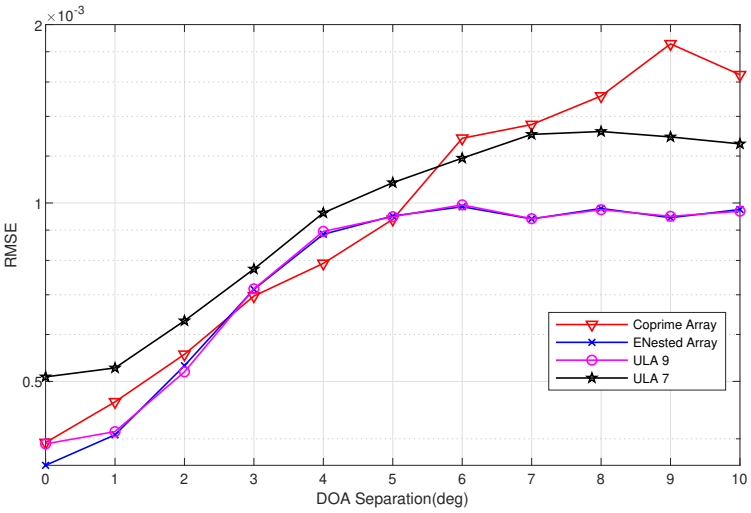

Fig. 5 RMSE versus the DOA separation of circular and non-circular signals with snapshot number 500.

6 Conclusion

In this paper, a gridless DOA estimation method has been proposed for a mixture of circular and non-circular signals by employing the recently proposed ENested array whose sum and difference co-arrays have no holes. The proposed method can successfully reconstruct the covariance matrix of the virtual signals of the sum and difference co-arrays based on atomic norm minimization and can still work well even when the circular and non-circular signals come from the same set of directions. As demonstrated by computer simulations, the

proposed method can achieve a performance close to the ULAs with the same physical aperture as the difference and sum combined virtual aperture of the employed ENested array.

Acknowledgement

This work is sponsored by the National Natural Science Foundation of China under Grant No. 61871282 and No. 62001256, the Key Laboratory of Intelligent Perception and Advanced Control of State Ethnic Affairs Commission under Grant MDIPAC-2019102, and by Zhejiang Provincial Natural Science Foundation of China under Grant No. LQ19F010002.

Data Availability Statement

The data included in this study may be available upon reasonable request by contacting with the corresponding author.

References

1. Bhaskar, B.N., Tang, G., Recht, B.: Atomic norm denoising with applications to line spectral estimation. IEEE Transactions on Signal Processing **61**(23), 5987–5999 (2013). DOI 10.1109/TSP.2013.2273443
2. Cai, J., Liu, W., Zong, R., Wu, B.: Sparse array extension for non-circular signals with subspace and compressive sensing based doa estimation methods. Signal Processing **145**, 59 – 67 (2018). DOI https://doi.org/10.1016/j.sigpro.2017.11.012
3. Chen, H., Hou, C., Liu, W., Zhu, W.P., Swamy, M.N.S.: Efficient two-dimensional direction-of-arrival estimation for a mixture of circular and noncircular sources. IEEE Sensors Journal **16**(8), 2527–2536 (2016). DOI 10.1109/JSEN.2016.2517128
4. Chen, H., Hou, C., Zhu, W.P., Liu, W., Dong, Y., Wang, Q.: Joint diagonalization based 2d doa estimation for mixed circular and strictly noncircular sources. In: 2017 IEEE Radar Conference (RadarConf), pp. 0001–0005 (2017). DOI 10.1109/RADAR.2017.7944160
5. Chen, H., Hou, C., Zhu, W.P., Liu, W., Dong, Y.Y., Peng, Z., Wang, Q.: Esprit-like two-dimensional direction finding for mixed circular and strictly noncircular sources based on joint diagonalization. Signal Processing **141**, 48 – 56 (2017). DOI https://doi.org/10.1016/j.sigpro.2017.05.024
6. Chen, H., Wang, W., Liu, W.: Joint doa, range, and polarization estimation for rectilinear sources with a cold array. IEEE Wireless Communications Letters **8**(5), 1398–1401 (2019). DOI 10.1109/LWC.2019.2919542
7. Chen, X., Zhang, X., Yang, J., Sun, M.: How to overcome basis mismatch: From atomic norm to gridless compressive sensing. Acta Automatica Sinica **42**(3), 335–346 (2016). DOI doi:10.16383/j.aas.2016.c150539
8. Chevalier, P., Blin, A.: Widely linear mvdr beamformers for the reception of an unknown signal corrupted by noncircular interferences. IEEE Transactions on Signal Processing **55**(11), 5323–5336 (2007)
9. Cohen, R., Eldar, Y.C.: Sparse convolutional beamforming for ultrasound imaging. IEEE Transactions on Ultrasonics, Ferroelectrics, and Frequency Control **65**(12), 2390–2406 (2018). DOI 10.1109/TUFFC.2018.2874256
10. Gao, F., Nallanathan, A., Wang, Y.: Improved music under the coexistence of both circular and noncircular sources. IEEE Transactions on Signal Processing **56**(7), 3033–3038 (2008). DOI 10.1109/TSP.2007.916123

11. Guo, M., Zhang, Y.D., Chen, T.: Doa estimation using compressed sparse array. IEEE Transactions on Signal Processing **66**(15), 4133–4146 (2018). DOI 10.1109/TSP.2018.2847645
12. Liu, A., Liao, G., Xu, Q., Zeng, C.: A circularity-based doa estimation method under coexistence of noncircular and circular signals. In: 2012 IEEE International Conference on Acoustics, Speech and Signal Processing (ICASSP), pp. 2561–2564 (2012). DOI 10.1109/ICASSP.2012.6288439
13. Liu, C., Vaidyanathan, P.: Super nested arrays: Linear sparse arrays with reduced mutual coupling—part ii: High-order extensions. IEEE Transactions on Signal Processing **64**(16), 4203–4217 (2016). DOI 10.1109/TSP.2016.2558167
14. Liu, C., Vaidyanathan, P.P.: Super nested arrays: Linear sparse arrays with reduced mutual coupling—part i: Fundamentals. IEEE Transactions on Signal Processing **64**(15), 3997–4012 (2016). DOI 10.1109/TSP.2016.2558159
15. Liu, C., Vaidyanathan, P.P., Pal, P.: Coprime coarray interpolation for doa estimation via nuclear norm minimization. In: 2016 IEEE International Symposium on Circuits and Systems (ISCAS), pp. 2639–2642 (2016). DOI 10.1109/ISCAS.2016.7539135
16. Liu, C.L., Vaidyanathan, P.: Cramér–rao bounds for coprime and other sparse arrays, which find more sources than sensors. Digital Signal Processing **61**, 43 – 61 (2017). DOI 10.1016/j.dsp.2016.04.011. Special Issue on Coprime Sampling and Arrays
17. Liu, Z., Huang, Z., Zhou, Y., Liu, J.: Direction-of-arrival estimation of noncircular signals via sparse representation. IEEE Transactions on Aerospace and Electronic Systems **48**(3), 2690–2698 (2012). DOI 10.1109/TAES.2012.6237619
18. Lustig, M., Donoho, D.L., Santos, J.M., Pauly, J.M.: Compressed sensing mri. IEEE Signal Processing Magazine **25**(2), 72–82 (2008). DOI 10.1109/MSP.2007.914728
19. Pal, P., Vaidyanathan, P.P.: Nested arrays: A novel approach to array processing with enhanced degrees of freedom. IEEE Transactions on Signal Processing **58**(8), 4167–4181 (2010). DOI 10.1109/TSP.2010.2049264
20. Picinbono, B., Chevalier, P.: Widely linear estimation with complex data. IEEE Transactions on Signal Processing **43**(8), 2030–2033 (1995)
21. Qin, G., Amin, M.G., Zhang, Y.D.: Doa estimation exploiting sparse array motions. IEEE Transactions on Signal Processing **67**(11), 3013–3027 (2019)
22. Qin, S., Zhang, Y.D., Amin, M.G.: Generalized coprime array configurations for direction-of-arrival estimation. IEEE Transactions on Signal Processing **63**(6), 1377–1390 (2015). DOI 10.1109/TSP.2015.2393838
23. Raza, A., Liu, W., Shen, Q.: Thinned coprime array for second-order difference co-array generation with reduced mutual coupling. IEEE Transactions on Signal Processing **67**(8), 2052–2065 (2019). DOI 10.1109/TSP.2019.2901380
24. Roy, R., Kailath, T.: Esprit-estimation of signal parameters via rotational invariance techniques. IEEE Transactions on Acoustics, Speech, and Signal Processing **37**(7), 984–995 (1989). DOI 10.1109/29.32276
25. Schmidt, R.: Multiple emitter location and signal parameter estimation. IEEE Transactions on Antennas and Propagation **34**(3), 276–280 (1986). DOI 10.1109/TAP.1986.1143830
26. Shen, Q., Liu, W., Cui, W., Wu, S., Zhang, Y.D., Amin, M.G.: Low-complexity direction-of-arrival estimation based on wideband co-prime arrays. IEEE/ACM Transactions on Audio, Speech, and Language Processing **23**(9), 1445–1456 (2015). DOI 10.1109/TASLP.2015.2436214
27. Steinwandt, J., Roemer, F., Haardt, M., Del Galdo, G.: Deterministic cramér-rao bound for strictly non-circular sources and analytical analysis of the achievable gains. IEEE Transactions on Signal Processing **64**(17), 4417–4431 (2016). DOI 10.1109/TSP.2016.2566603
28. Steinwandt, J., Roemer, F., Haardt, M., Galdo, G.D.: R-dimensional esprit-type algorithms for strictly second-order non-circular sources and their performance analysis. IEEE Transactions on Signal Processing **62**(18), 4824–4838 (2014). DOI 10.1109/TSP.2014.2342673
29. Stoica, P., Larsson, E.G., Gershman, A.B.: The stochastic crb for array processing: a textbook derivation. IEEE Signal Processing Letters **8**(5), 148–150 (2001). DOI 0.1109/97.917699

30. Tang, G., Bhaskar, B.N., Shah, P., Recht, B.: Compressed sensing off the grid. IEEE Transactions on Information Theory **59**(11), 7465–7490 (2013). DOI 10.1109/TIT.2013.2277451
31. Teng, L., Wang, Q., Chen, H., Zhu, W., Liu, W., Cai, J.: Doa estimation for coexistence of circular and non-circular signals based on atomic norm minimization. In: 2020 IEEE 11th Sensor Array and Multichannel Signal Processing Workshop (SAM), pp. 1–5 (2020). DOI 10.1109/SAM48682.2020.9104368
32. Vaidyanathan, P.P., Pal, P.: Sparse sensing with co-prime samplers and arrays. IEEE Transactions on Signal Processing **59**(2), 573–586 (2011). DOI 10.1109/TSP.2010.2089682
33. Wang, Q., Wang, X., Chen, H., Zhu, X., Liu, W., Yan, W., Wang, L.: An effective localization method for mixed far-field and near-field strictly non-circular sources. Digital Signal Processing **94**, 125 – 136 (2019). DOI https://doi.org/10.1016/j.dsp.2019.06.003. Special Issue on Source Localization in Massive MIMO
34. Wang, X., Chen, Z., Ren, S., Cao, S.: Doa estimation based on the difference and sum coarray for coprime arrays. Digital Signal Processing **69**, 22 – 31 (2017). DOI https://doi.org/10.1016/j.dsp.2017.06.013. URL `http://www.sciencedirect.com/science/article/pii/S1051200417301276`
35. Wang, X., Wan, L., Huang, M., Shen, C., Zhang, K.: Polarization channel estimation for circular and non-circular signals in massive mimo systems. IEEE Journal of Selected Topics in Signal Processing **13**(5), 1001–1016 (2019). DOI 10.1109/JSTSP.2019.2925786
36. Wu, X., Zhu, W.P., Yan, J.: A toeplitz covariance matrix reconstruction approach for direction-of-arrival estimation. IEEE Transactions on Vehicular Technology **66**(9), 8223–8237 (2017). DOI 10.1109/TVT.2017.2695226
37. Wu, X., Zhu, W.P., Yan, J.: A high-resolution doa estimation method with a family of nonconvex penalties. IEEE Transactions on Vehicular Technology **67**(6), 4925–4938 (2018). DOI 10.1109/TVT.2018.2817638
38. X.Wu, Zhu, W.P., Yan, J.: Gridless two-dimensional doa estimation with l-shaped array based on the cross-covariance matrix. In: 2018 IEEE International Conference on Acoustics, Speech and Signal Processing (ICASSP), pp. 3256–3260 (2018). DOI 10.1109/ICASSP.2018.8461481
39. Zheng, Z., Huang, Y., Wang, W.Q., So, H.C.: Direction-of-arrival estimation of coherent signals via coprime array interpolation. IEEE Signal Processing Letters **27**, 585–589 (2020). DOI 10.1109/LSP.2020.2982769
40. Zheng, Z., Mu, S.: Two-dimensional doa estimation using two parallel nested arrays. IEEE Communications Letters **24**(3), 568–571 (2020). DOI 10.1109/LCOMM.2019.2958903
41. Zheng, Z., Wang, W., Kong, Y., Zhang, Y.D.: Misc array: A new sparse array design achieving increased degrees of freedom and reduced mutual coupling effect. IEEE Transactions on Signal Processing **67**(7), 1728–1741 (2019). DOI 10.1109/TSP.2019.2897954
42. Zhou, C., Gu, Y., Fan, X., Shi, Z., Mao, G., Zhang, Y.D.: Direction-of-arrival estimation for coprime array via virtual array interpolation. IEEE Transactions on Signal Processing **66**(22), 5956–5971 (2018). DOI 10.1109/TSP.2018.2872012
43. Zhou, C., Gu, Y., He, S., Shi, Z.: A robust and efficient algorithm for coprime array adaptive beamforming. IEEE Transactions on Vehicular Technology **67**(2), 1099–1112 (2018). DOI 10.1109/TVT.2017.2704610